



Atomic and Molecular Effects on Spherically Convergent Ion Flow I: Single Atomic Species

G.A. Emmert and J.F. Santarius

July 2009

UWFDM-1369

Published in *Physics of Plasmas* 17, 013502 (2010).

FUSION TECHNOLOGY INSTITUTE

UNIVERSITY OF WISCONSIN

MADISON WISCONSIN

Atomic and Molecular Effects on Spherically Convergent Ion Flow I: Single Atomic Species

G.A. Emmert and J.F. Santarius

Fusion Technology Institute
University of Wisconsin
1500 Engineering Drive
Madison, WI 53706

<http://fti.neep.wisc.edu>

July 2009

UWFDM-1369

Published in *Physics of Plasmas* 17, 013502 (2010).

Atomic and molecular effects on spherically convergent ion flow I: single atomic species

G. A. Emmert and J. F. Santarius
*Fusion Technology Institute, University of Wisconsin-Madison,
1500 Engineering Drive,
Madison, Wisconsin 53706, USA
santarius@engr.wisc.edu*

ABSTRACT

A formalism for analyzing the effect of ion-neutral gas interactions on the flow of ions between nearly transparent electrodes in spherical geometry has been developed for atomic ions in a weakly ionized plasma, so that the important atomic effects are charge exchange and ion impact ionization. The formalism is applied to spherical, gridded, inertial-electrostatic confinement (IEC) devices. The formalism yields detailed information about the energy spectra of the ions and fast neutral atoms, and the resulting fusion rate for ^3He ions in a background ^3He gas. The results are illustrated with an example calculation for the Wisconsin IEC device operating on ^3He .

I. INTRODUCTION

Investigations of charged-particle flow between electrodes date back to Child¹ and Langmuir,² and the problem possesses a long history^{3,4,5,6,7,8,9} that continues today.^{10,11} The Child-Langmuir problem has been solved for completely ionized plasmas, but the presence of neutral gas and multiple species complicates the analysis. The present paper addresses the problem of spherically convergent ion flow of a single, atomic species at moderate pressure ($>0.133\text{ Pa} = 1\text{ mTorr}$) in a weakly ionized plasma, where the effects of charge exchange and ionization must be included. The results will apply to singly charged helium flow,^{12,13} for example. A companion paper¹⁴ extends the analysis to the problem of multiple molecular species, which is more generally applicable but substantially more complicated. The theory developed herein applies to ion flow in spherical geometry between solid electrodes, and also to a configuration called gridded *inertial-electrostatic confinement* (IEC),^{15,16,17} in which ions make multiple radial passes between nearly transparent electrodes.

Most present IEC experiments operate in the moderate-pressure regime.^{18,19,20,21,22,23,24,25} Several active IEC experimental efforts exist, including devices at the University of Wisconsin,^{24,26} University of Illinois,¹⁸ Los Alamos National Laboratory,²⁷ University of Missouri—Columbia,²⁸ Kyoto University,²³ Kansai University,²³ Kyushu University,²³ and Tokyo Institute of Technology.²³ The main motivation for recent IEC research has been to create fusion-product neutrons and protons for use in detecting landmines²³ and highly enriched uranium,²⁹ producing radioisotopes,³⁰ and pursuing other applications.³¹ The present paper and its companion paper aim to provide tools for understanding ion flow at moderate pressures. We anticipate that the theory will also be useful for the optimization of such devices.

The theoretical framework for the problem is laid in Sec. II. As an example calculation, Sec. III gives some results for ^3He operation in the Wisconsin IEC device.

II. THEORETICAL MODEL

A. Overview

For a nearly transparent inner electrode in spherically symmetric geometry, ions accelerated inward by the electric field pass through the inner electrode (cathode) and experience multiple passes between the region near the origin and the outer electrode (anode). The ion flow problem consists of analyzing ion interactions (charge exchange and ionization of background gas, plus collisions with grid wires) during their radial bounce motion in the electrostatic potential well. For the case of a single atomic species, charge exchange reactions generate a fast neutral atom and a cold ion, whereas ionization of background gas creates a cold ion. The cold ions created by charge exchange and ionization are considered to belong to the next ion generation; in the case of charge exchange the parent ion disappears, causing attenuation of the parent generation. The electrostatic potential difference accelerates cold ions, producing energetic ions that can interact with the background gas to produce new fast neutral atoms and cold ions. The integral equation analysis presented here follows this infinite recursion of generations of ions. The key physics effects in gridded IEC devices are illustrated in Fig. 1 for the moderate-pressure regime of the experiments.

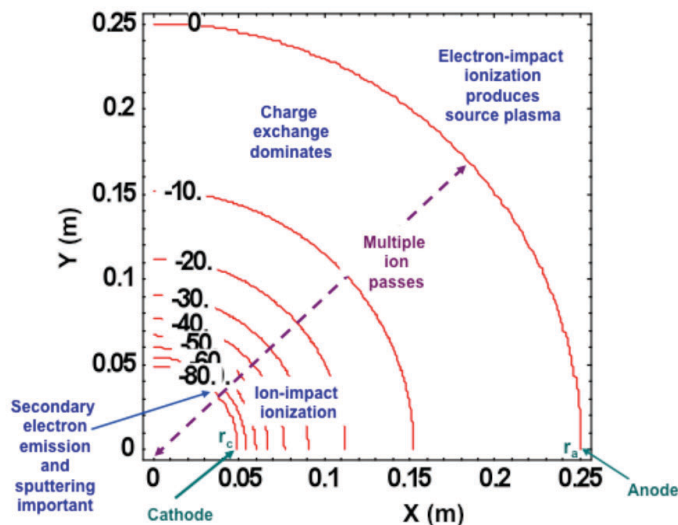


Figure 1. Key features of inertial-electrostatic confinement physics. Contours shown are of the electrostatic potential. Only one quarter of the equatorial plane of the spherically symmetric geometry is shown.

In principal, the self-consistent radial electrostatic potential profile can be determined by the solution to Poisson's equation with the appropriate boundary conditions. For typical steady-state IEC device operation, the current is small compared with the space-charge-limited current, and the ion space charge does not significantly affect the vacuum electrostatic potential profile. The present analysis assumes that the radial electrostatic potential profile can be specified as an input to the analysis, rather than solved for self-consistently. The following definitions and assumptions will be used:

1. The spherically symmetric case is treated, ignoring the high-voltage, insulating stalk that separates the electrodes in experimental devices.
2. The cathode grid is at radius $r = a$, the anode is at radius $r = b$, and the cathode and anode transparencies are T_c and T_a , respectively.
3. The electrostatic potential, $\phi(r)$, is given, not solved for self-consistently. The electrostatic potential is assumed to be monotonically decreasing towards the cathode, which is at a large negative potential, and have negligible gradient inside the cathode region ($r < a$).
4. The cold neutral gas density, n_g , is uniform. In this paper, we consider only a single species of neutrals and ions with charge q .
5. The plasma is assumed to be weakly ionized.
6. We consider charge exchange and ionization between the ions and the cold background gas as the only atomic processes. We assume that the fast neutral atoms produced by charge exchange reach the walls of the IEC device without interaction (except for fast neutral atoms striking gas atoms and producing fusion reactions), so we ignore them after they are created and focus on the birth of cold ions by charge exchange. Ionization by ion impact is assumed to occur with little momentum transfer, so that the incident ion is not slowed and the newly created ion is cold.
7. Ionization and charge exchange inside the cathode region ($r < a$) produce cold ions that are electrostatically trapped; they wander around the cathode region and ultimately hit the cathode grid or are neutralized by trapped electrons in that region. We neglect any acceleration of these ions by the potential since the gradients are assumed small inside the cathode region.

Summing over an infinite number of radial passes and generations of ions results in a Volterra integral equation for the source of cold ions. From this source function, the energy spectrum of the ions and energetic neutrals is obtained, along with other macroscopic quantities of interest. The numerical solution of the Volterra integral equation for helium and atomic deuterium has been implemented in a computer code used to generate the results in Sec. III.

B. Volterra equation for the ion source function

We divide the ions into two classes, class I ions and class II ions. Class I ions are created in the source region outside the anode and cross the anode grid heading towards the cathode. Class II ions are ions created in the region between the anode and cathode (the intergrid region). Class I ions may undergo charge exchange and thereby become the source of class II ions. They can also ionize the background gas, which adds to the source of class II ions. Class II ions, which are born at radius $r < b$ due to charge exchange and ionization, accelerate inwards and, upon reaching the origin, become outgoing ions that reflect at their birth radius and start a new pass towards the origin. We divide class II ions into generations, with charge exchange and impact on the grid wires being the loss processes for a given generation, and charge exchange and ionization being the source of the next generation.

As class I ions leave the anode and head inward they are attenuated by charge exchange; the probability of surviving to reach the radius r is

$$f(r) = \exp \left\{ - \int_r^b n_g \sigma_{cx} [E(r')] dr' \right\} \quad (1)$$

where the charge exchange cross section, σ_{cx} , is a function of the energy, E , of the ion,

$$E(r') = E_0 - q\phi(r'). \quad (2)$$

The ions have been assumed to leave the anode with the (small) energy E_0 . The non-directed flux (sum of the inward and outward fluxes) of class I ions at radius r (for $a < r < b$) is

$$\Gamma(r) = \frac{b^2\Gamma_0}{r^2} \left[f(r) + T_c^2 \frac{f^2(0)}{f(r)} \right], \quad (3)$$

where Γ_0 is the flux of ions crossing the anode and heading inward. The first term, $f(r)$, in Eq. (3) is the contribution of the inward traveling class I ions to the flux at radius r ; those ions that made it this far have a certain probability of passing through the cathode and reaching the radius r on their way back to the anode; the second term, $T_c^2 f^2(0)/f(r)$, measures their contribution to the flux at r on their way out. The factor T_c^2 is because they passed through the cathode grid twice. To see that the survival factor for the returning ions can be put in this form, note that the survival factor (not including the cathode transparency) for a transit from the anode to the origin and then back to r is

$$\exp\left(-\int_0^b n_g \sigma_{cx} dr' - \int_0^r n_g \sigma_{cx} dr'\right) = \exp\left(-2\int_0^b n_g \sigma_{cx} dr' + \int_r^b n_g \sigma_{cx} dr'\right) = \frac{f^2(0)}{f(r)}, \quad (4)$$

where

$$f^2(0) = \exp\left(-2\int_0^b n_g \sigma_{cx} dr'\right) \quad (5)$$

is the probability of making a complete pass from the anode back to the anode. We do not follow class I ions beyond one complete pass through the cathode and back to the anode. Those ions that reach the anode are assumed to rejoin the reservoir of ions in the source region outside the anode.

The ionization and charge exchange rate at radius r is

$$A(r) = n_g \Gamma(r) \sigma_{tot}[E(r)], \quad (6)$$

where σ_{tot} is the total cross section,

$$\sigma_{tot} = \sigma_{cx} + \sigma_{ioniz}, \quad (7)$$

and σ_{ioniz} is the ion impact ionization cross section. Using Eq. (3), we get

$$A(r) = \frac{b^2 n_g \sigma_{tot}[E(r)]}{r^2} \left[f(r) + T_c^2 \frac{f^2(0)}{f(r)} \right]. \quad (8)$$

We divide class II ions into generations. Ionization and charge exchange of class I ions with the background gas [Eq.(8)] constitute the sources of the first generation of class II ions. These ions are born cold and are accelerated towards the origin by the electric field. Each generation will travel continually from their birth radius through the cathode and back to their birth radius, where they reflect and start another pass, until they undergo charge exchange or hit the cathode grid. Hence we have to sum over an infinite number of passes. These ions create the next generation by charge exchange and ionization with the background gas. Hence we also have to sum over an infinite number of generations to get the total ion density.

Consider a source shell at radius r' . The energy at radius r of the ions born at radius r' is

$$E(r, r') = q \phi(r') - q \phi(r). \quad (9)$$

We define the survival function

$$g(r, r') = \exp \left\{ - \int_r^{r'} n_g \sigma_{cx} [E(r'', r')] dr'' \right\} \quad (10)$$

which measures the probability of an ion born at radius r' reaching the radius r . The contribution to the non-directed flux at r due to ions born in the shell at r' is

$$d\Gamma(r) = \begin{cases} \frac{A(r') r'^2 dr'}{r^2} \left[g(r, r') + T_c^2 \frac{g^2(0, r')}{g(r, r')} \right] & r < r' \\ 0, & r > r' \end{cases} \quad (11)$$

The first term in the square brackets in Eq. (11) is the contribution from inward-traveling ions born at r' and traveling to r . The second term is the contribution from ions born at r' that penetrated to the origin and are now traveling outward at r . This form for the attenuation factor is obtained by the same arguments used for class I ions. However, the ions that survive all the way back to the birth radius can make additional passes through the shell at r and thus contribute again to the flux at r . We define the complete pass attenuation factor

$$g_{cp}(r') = g^2(0, r'). \quad (12)$$

Each pass is attenuated by $T_c^2 g_{cp}(r')$ compared with the previous pass, so summing over passes gives the contribution,

$$1 + T_c^2 g_{cp} + (T_c^2 g_{cp})^2 + (T_c^2 g_{cp})^3 + (T_c^2 g_{cp})^4 + \dots = \frac{1}{1 - T_c^2 g_{cp}(r')}, \quad (13)$$

so that the flux in the shell at r due to the ions born at r' becomes

$$d\Gamma(r) = \begin{cases} \frac{A(r') r'^2 dr'}{r^2} \left[g(r, r') + T_c^2 \frac{g_{cp}(r')}{g(r, r')} \right] \frac{1}{1 - T_c^2 g_{cp}(r')}, & r < r' \\ 0, & r > r' \end{cases} \quad (14)$$

The production rate of cold ions by charge exchange and ionization at r due to ions that were born at r' is

$$dS_1(r) = d\Gamma(r) n_g \sigma_{tot} [E(r, r')]. \quad (15)$$

Substituting from Eq. (14) and integrating over the radius r' , we get the source rate for the next generation of class II ions at radius r ;

$$S_1(r) = \int_0^b K(r, r') A(r') dr', \quad (16)$$

where the kernel $K(r, r')$ is defined by

$$K(r, r') = \begin{cases} n_g \sigma_{tot} [E(r, r')] \left(\frac{r'^2}{r^2} \right) \left[g(r, r') + T_c^2 \frac{g_{cp}(r')}{g(r, r')} \right] \frac{1}{1 - T_c^2 g_{cp}(r')}, & r < r' \\ 0, & r > r' \end{cases} \quad (17)$$

Now consider subsequent generations, letting p denote the generation number. For the $p+1$ generation, which is born by charge exchange and ionization from the p th generation, we have

$$S_{p+1}(r) = \int_0^b K(r, r') S_p(r') dr', \quad p=1, 2, \dots, \infty, \quad (18)$$

by the same reasoning that led to Eq. (16). Note that the kernel K is independent of the generation number. It is convenient to write Eq. (18) symbolically as

$$S_{p+1}(r) = K S_p(r), \quad p=1, 2, \dots, \infty, \quad (19)$$

where K is the integral operator whose kernel is defined by Eqs. (17), and $S_1(r)$ is defined by Eq. (16). The total source rate at r due to class I ions and all generations of class II ions is

$$S(r) = A(r) + \sum_{p=1}^{\infty} S_p(r). \quad (20)$$

Using operator notation and applying Eq. (18) recursively gives

$$S(r) = [I + K + K^2 + K^3 + \dots] A(r) = \frac{1}{I - K} A(r), \quad (21)$$

where I is the identity operator. We can rewrite this as

$$S(r) = A(r) + K S(r) = A(r) + \int_a^b K(r, r') S(r') dr', \quad (22)$$

where we have replaced the operator K by its definition in terms of the kernel $K(r, r')$. Eq. (22) is an integral equation for the source rate. It is written in the Fredholm form, but it is actually a Volterra integral equation since the kernel is zero for $r > r'$. The Volterra form is

$$S(r) = A(r) + \int_r^b K(r, r') S(r') dr'. \quad (23)$$

Eq. (23) can be solved by finite difference methods³².

C. Energy spectra

1. Energy spectrum of the fast ion flux for $r > a$

We now turn our attention to the energy spectrum, $f(r, E)$, in the region between the anode and the cathode. We define $f(r, E)$ to be the energy spectrum of the particle flux at radius r , so that $\int f(r, E) dE$ is the particle flux passing radius r in a given direction. Since we have inward-going ions and outward-going ions, we introduce an energy spectrum for each, i.e. $f^-(r, E)$ and $f^+(r, E)$. Consider a shell of thickness dr' at radius r' and a surface at radius r . For inward moving ions,

$$4\pi r^2 f^-(r, E) dE = S(r') \frac{g(r, r')}{1 - T_c^2 g_{cp}(r')} 4\pi r'^2 dr', \quad (24)$$

where $E = E(r, r')$ is given in Eq. (9). Differentiating Eq. (9) with respect to r' , we obtain the relationship between the “window widths” dr' and dE ,

$$dE = q \left| \frac{\partial \phi}{\partial r'} \right| dr'. \quad (25)$$

We introduced the absolute value signs since both dE and dr' are considered positive. Thus the

energy distribution of fast ions is

$$f^-(r, E) = \left(\frac{1}{q} \right) \left(\frac{r'}{r} \right)^2 \frac{S(r')}{\left| \frac{\partial \phi}{\partial r'} \right|} \left[\frac{g(r, r')}{1 - T_c^2 g_{cp}(r')} \right] \quad (26)$$

for inward moving ions.

For outward moving ions we replace $g(r, r')$ by the survival function for ions that have traversed the core and are heading outward, giving

$$f^+(r, E) = \left(\frac{1}{q} \right) \left(\frac{r'}{r} \right)^2 \frac{S(r')}{\left| \frac{\partial \phi}{\partial r'} \right|} \left[\frac{T_c^2 g_{cp}(r')}{1 - T_c^2 g_{cp}(r')} \right] \frac{1}{g(r, r')}. \quad (27)$$

Equations (26) and (27) apply for ion energies less than the full potential difference between the anode and the point where we are evaluating the distribution function. We also need to include the class I ions at the full (local) energy. Using Eqs. (2) and (3), we add the class I beam-like contribution by introducing the delta function. For inward traveling ions, the energy spectrum is

$$f^-(r, E) = \left(\frac{1}{q} \right) \left(\frac{r'}{r} \right)^2 \frac{S(r')}{\left| \frac{\partial \phi}{\partial r'} \right|} \left[\frac{g(r, r')}{1 - T_c^2 g_{cp}(r')} \right] + \frac{b^2 \Gamma_0 f(r)}{r^2} \delta[E - E_0 - q \phi(r)], \quad (28)$$

and, for outward moving ions, it is

$$f^+(r, E) = \left(\frac{1}{q} \right) \left(\frac{r'}{r} \right)^2 \frac{S(r')}{\left| \frac{\partial \phi}{\partial r'} \right|} \left[\frac{T_c^2 g_{cp}(r')}{1 - T_c^2 g_{cp}(r')} \right] \frac{1}{g(r, r')} + \frac{b^2 \Gamma_0 T_c^2 f^2(0)}{r^2 f(r)} \delta[E - E_0 - q \phi(r)] \quad (29)$$

In Eq. (28) and (29), the radius r' is restricted to $r < r' < b$, so that Eq. (9) has a positive solution for the energy E .

2. Energy spectrum of the fast ion flux for $r < a$

We can also evaluate the energy spectrum of the fast ion flux inside the cathode region ($r < a$). The source of these ions is the same as for the intergrid region, but we have to include the loss due to impact on the cathode grid in passing into the cathode region. The result is

$$f^-(r, E) = \left(\frac{1}{q} \right) \left(\frac{r'}{r} \right)^2 \frac{S(r')}{\left| \frac{\partial \phi}{\partial r'} \right|} T_c \left[\frac{g(r, r')}{1 - T_c^2 g_{cp}(r')} \right] + \frac{b^2 \Gamma_0 T_c f(r)}{r^2} \delta[E - E_0 - q \phi(a)], \quad (30)$$

for inward traveling ions, and

$$f^+(r, E) = \left(\frac{1}{q} \right) \left(\frac{r'}{r} \right)^2 \frac{S(r')}{\left| \frac{\partial \phi}{\partial r'} \right|} \left[\frac{T_c g_{cp}(r')}{1 - T_c^2 g_{cp}(r')} \right] \frac{1}{g(r, r')} + \frac{b^2 \Gamma_0 T_c f^2(0)}{r^2 f(r)} \delta[E - E_0 - q \phi(a)] \quad (31)$$

for outward traveling ions.

The ions in the cathode region travel at constant energy since the potential is assumed to be constant. Hence, the survival functions $f(r)$ and $g(r, r')$ can be written as

$$f(r) = f(a) \exp\{n_g \sigma_{cx} [E(a)] (r - a)\}, \quad (32)$$

$$g(r, r') = g(a, r') \exp\{n_g \sigma_{cx} [E(a, r')](r - a)\}. \quad (33)$$

Note that the radius r' in Eqs. (30), (31), and (33) is restricted to $a < r' < b$, since the class II ions are born in the intergrid region.

3. *Energy spectrum of the fast neutral atom flux*

Ions of energy E undergoing charge exchange produce fast atoms; we determine the energy spectra of the fast atoms by determining the energy of the ions that created them. We start with a flux of class I ions with energy E_0 leaving the anode surface of radius b and heading inward. The ions are accelerated by the potential and therefore have kinetic energy E , given by Eq. (2), at the radius r' , creating fast neutral atoms at radius r' with energy E . The number of fast neutrals created per unit time per unit volume at radius r' is

$$S_{n1}(r') = n_g \Gamma(r') \sigma_{cx}(E). \quad (34)$$

Substituting for the inward flux [see Eq. (3)], we get

$$S_{n1}(r') = n_g \sigma_{cx}(E) \frac{b^2}{r'^2} \Gamma_0 f(r'). \quad (35)$$

This volume source of fast neutrals will produce a flux of fast neutrals of energy E at a radius r , where $r < r'$. We write the fast neutral flux as

$$\Gamma_{n1}^{\pm}(r) = \int f_{n1}^{\pm}(r, E) dE, \quad (36)$$

where $f^{\pm}(r, E)$ is the energy spectrum of the fast neutral atom flux. The + or – superscript denotes the direction of travel of the neutral atoms. The “1” in the subscript denotes that these neutrals were generated by charge exchange of class I ions. The neutral atoms arriving at radius r with energy inside a window dE about E all came from a spherical shell of radius r' and thickness dr' . Consequently,

$$4\pi r^2 f_{n1}^-(r, E) dE = 4\pi r'^2 S_{n1}(r') dr'. \quad (37)$$

Substituting from Eq. (35) we get

$$f_{n1}^-(r, E) dE = \frac{b^2}{r^2} n_g \sigma_{cx}(E) \Gamma_0 f(r') dr', \quad (38)$$

where E and r' are related by Eq. (2). Differentiating Eq. (2), we get

$$dE = q \left| \frac{\partial \phi(r')}{\partial r'} \right| dr'. \quad (39)$$

The absolute value sign has been introduced so that the “window widths” dE and dr' are both positive. Inserting Eq. (39) into Eq. (38), we get

$$f_{n1}^-(r, E) = \frac{b^2}{r^2 q \left| \frac{\partial \phi(r')}{\partial r'} \right|} n_g \sigma_{cx}(E) \Gamma_0 f(r') \Theta(r' - r), \quad r < a < r'. \quad (40)$$

This expression gives the energy spectrum of the fast neutral atoms traveling inward. Note that the r' in Eq. (40) is an implicit function of E through Eq. (2). If Eq. (2) has no solution for a

certain E , then the corresponding $f_{n1}^-(r, E)$ is zero. We have introduced the Heaviside step function Θ into Eq. (40); it forces $r' > r$.

Inside the cathode region, the result corresponding to Eq. (40) is

$$f_{n1}^-(r, E) = \frac{b^2}{r^2 q \left| \frac{\partial \phi(r')}{\partial r'} \right|} n_g \sigma_{cx}(E) T_c \Gamma_0 f(r'), \quad r < a < r'. \quad (41)$$

The factor T_c enters because of the attenuation of the fast neutrals while crossing the grid. Note that Eq. (41) considers only the fast neutrals that arose from charge exchange in the intergrid region. Because of the potential variation at the point of charge exchange, the energy spectrum is continuous, not discrete. Since our model for the potential assumes a constant potential inside the cathode, charge exchange inside the cathode region gives rise to a discrete spectrum of fast neutrals at the full ion energy,

$$E_{\max} = E_0 = q \phi(a). \quad (42)$$

The inward flux of ions just inside the cathode is

$$\Gamma_i^-(a) = \frac{b^2}{a^2} T_c \Gamma_0 f(a). \quad (43)$$

As these ions traverse the cathode region some of them undergo charge exchange to become fast neutrals. At radius r the ion flux is

$$\Gamma_i^-(r) = \frac{a^2}{r^2} \Gamma_i^-(a) \exp[n_g \sigma_{cx}(E_{\max})(r-a)], \quad (44)$$

where the exponential term arises because of attenuation by charge exchange between r and a . Since particles are conserved by this process,

$$\Gamma_{n1}^-(r) + \Gamma_i^-(r) = \frac{a^2}{r^2} \Gamma_i^-(a), \quad (45)$$

so that the fast neutral flux arising from charge exchange inside the cathode is

$$\Gamma_{n1}^-(r) = \frac{b^2}{r^2} T_c \Gamma_0 f(a) \left\{ 1 - \exp[n_g \sigma_{cx}(E_{\max})(r-a)] \right\}. \quad (46)$$

Equations (41) and (46) can be combined into one expression by introducing the delta function. We get

$$f_{n1}^-(r, E) = \frac{b^2}{r^2 q \left| \frac{\partial \phi(r')}{\partial r'} \right|} n_g \sigma_{cx}(E) T_c \Gamma_0 f(r') + \frac{b^2}{r^2} T_c \Gamma_0 f(a) \left\{ 1 - \exp[n_g \sigma_{cx}(E_{\max})(r-a)] \right\} \delta(E - E_{\max})$$

for $r < a < r'$.

The inward traveling fast neutrals cross the origin and become outward traveling fast neutrals. We also pick up a contribution from charge exchange of outward traveling ions with background gas. We start with the region inside the cathode and consider the discrete spectrum. From particle conservation,

$$\Gamma_{n1}^-(r) + \Gamma_i^-(r) = \Gamma_{n1}^+(r) + \Gamma_i^+(r). \quad (48)$$

But

$$\Gamma_i^+(r) = \Gamma_i^-(r) \exp[-2n_g \sigma_{cx}(E_{\max})], \quad (49)$$

so that, after using Eqs. (43)-(45) and (49), we get

$$\Gamma_{n1}^+(r) = \frac{b^2}{r^2} T_c \Gamma_0 f(a) \left\{ 1 - \exp[-n_g \sigma_{cx}(E_{\max})(a+r)] \right\}. \quad (50)$$

Adding in the continuous spectrum, which is unaffected by charge exchange in the cathode region, gives the final result,

$$\begin{aligned} f_{n1}^+(r, E) = & \frac{b^2}{r^2 q \left| \frac{\partial \phi(r')}{\partial r'} \right|} n_g \sigma_{cx}(E) T_c \Gamma_0 f(r') \\ & + \frac{b^2}{r^2} T_c \Gamma_0 f(a) \left\{ 1 - \exp[-n_g \sigma_{cx}(E_{\max})(a+r)] \right\} \delta(E - E_{\max}) \end{aligned} \quad (51)$$

for $r < a < r'$.

Next we consider the outgoing neutrals in the intergrid region ($a < r < b$); there will be both a continuous spectrum (due to the continuous spectrum of inward traveling neutrals and the additional charge exchange of outward traveling ions between the cathode and the point of interest) and a discrete spectrum (at the full energy) arising from charge exchange inside the cathode region. The current in the discrete part of the spectrum is attenuated by the cathode grid and then remains constant for larger r . For the discrete part of the spectrum,

$$\Gamma_{n1}^+(r) = \frac{b^2}{r^2} T_c^2 \Gamma_0 f(a) \left\{ 1 - \exp[-2n_g \sigma_{cx}(E_{\max})a] \right\}. \quad (52)$$

The continuous part of the spectrum can be written

$$f_{n1}^+(r, E) = T_c^2 f_{n1}^-(r, E) + \delta f_{n1}^+(r, E), \quad (53)$$

where δf is the contribution due to charge exchange of outward going ions with energy E . By the same arguments that led to Eq. (40) we get

$$\delta f_{n1}^+(r, E) = \frac{b^2}{r^2 q \left| \frac{\partial \phi(r')}{\partial r'} \right|} n_g \sigma_{cx}(E) T_c^2 \Gamma_0 \frac{f^2(0)}{f(r')}. \quad (54)$$

In this expression, the radius r' is restricted to $a < r' < r < b$. Putting these results together, we get

$$\begin{aligned} f_{n1}^+(r, E) = & \frac{b^2}{r^2 q \left| \frac{\partial \phi(r')}{\partial r'} \right|} n_g \sigma_{cx}(E) T_c^2 \Gamma_0 \left[f(r') + \frac{f^2(0)}{f(r')} \Theta(r-r') \right] \\ & + \frac{b^2}{r^2} T_c^2 \Gamma_0 f(a) \left\{ 1 - \exp[-2n_g \sigma_{cx}(E_{\max})a] \right\} \delta(E - E_{\max}) \end{aligned} \quad (55)$$

for $r < a < r'$. In this result, r' is an implicit function of E through Eq. (2).

We now consider fast neutrals generated by class II ions; these are born within the intergrid region. Consider a set of cold ions born within a shell of radius r'' and thickness dr'' . They travel inward and undergo charge exchange within a shell of radius r' and thickness dr' . Fast neutrals are emitted in the inward direction with energy E ,

$$E(r, r'') = q\phi(r'') - q\phi(r'). \quad (56)$$

Note that different sets of radii r' and r'' can produce fast neutrals with the same energy $E(r', r'')$ as long as they satisfy Eq. (56). Hence, to get the total fast neutral flux at a given energy, we have to integrate over possible source shells, i.e. integrate over r'' . We use the same formalism as for class I ions to describe the energy spectrum of the fast neutrals, but with the following replacements:

$$\begin{aligned} b^2 \Gamma_0 &\rightarrow r''^2 S(r'') dr'', \\ E(r') &\rightarrow E(r', r''), \\ f(r') &\rightarrow \frac{g(r', r'')}{1 - T_c^2 g_{cp}(r'')}. \end{aligned}$$

Thus, Eq. (40) becomes

$$df_{n_2}^-(r, E) = \frac{r''^2}{r^2 q \left| \frac{\partial \phi(r')}{\partial r'} \right|} n_g \sigma_{cx}(E) \frac{g(r', r'')}{1 - T_c^2 g_{cp}(r'')} S(r'') dr'' \quad (57)$$

Integrating this over r'' gives the result

$$f_{n_2}^-(r, E) = \frac{n_g \sigma_{cx}(E)}{r^2 q} \int_r^b \frac{S(r'')}{\left| \frac{\partial \phi(r')}{\partial r'} \right|} \left[\frac{g(r', r'')}{1 - T_c^2 g_{cp}(r'')} \right] \Theta(r' - r) r''^2 dr'' \quad (58)$$

For a given energy E , the radius r' is a function of r'' and E through Eq. (56). This variation has to be included in the integration over r'' . The Θ function was introduced to zero the integrand when $r' < r$; the inward traveling fast neutrals are born from inward traveling ions that were born at a larger radius.

Inside the cathode region, the corresponding equation is

$$f_{n_2}^-(r, E) = T_c \frac{n_g \sigma_{cx}(E)}{r^2 q} \int_a^b \frac{S(r'')}{\left| \frac{\partial \phi(r')}{\partial r'} \right|} \left[\frac{g(r', r'')}{1 - T_c^2 g_{cp}(r'')} \right] \Theta(r' - a) r''^2 dr'' \quad (59)$$

Eq. (59) assumes that the source of ions and the charge exchange process producing the fast neutrals are both located in the intergrid region.

We also have to add the fast neutrals born inside the cathode by charge exchange of class II ions traversing the cathode region. We use the same reasoning as for class I ions. Starting with Eq. (46) and making the replacements listed above, the fast neutral flux at r in a given energy range is

$$\delta \Gamma_{n_2}^-(r, E) = \frac{r''^2}{r^2} T_c S(r'') dr'' \left[\frac{g(a, r'')}{1 - T_c^2 g_{cp}(r'')} \right] \left\{ 1 - \exp[n_g \sigma_{cx}(E)(r - a)] \right\} \quad (60)$$

We let

$$\delta \Gamma_{n_2}^\pm(r, E) = f_{n_2}^\pm(r, E) dE, \quad (61)$$

where E is given by

$$E = q \phi(r'') - q \phi(a), \quad (62)$$

and the energy and spatial “window widths” are related by

$$dE = q \left| \frac{\partial \phi(r'')}{\partial r''} \right| dr''. \quad (63)$$

Our result becomes

$$f_{n2}^-(r, E) = \frac{r''^2}{r^2} T_c \left[\frac{g(a, r'')}{1 - T_c^2 g_{cp}(r'')} \right] \left\{ 1 - \exp[n_g \sigma_{cx}(E)(r - a)] \right\} \frac{S(r'')}{q \left| \frac{\partial \phi(r'')}{\partial r''} \right|}. \quad (64)$$

This contribution is in addition to the contribution in Eq. (59). Adding them together, we get the final result for inward traveling neutrals in the cathode region,

$$f_{n2}^-(r, E) = T_c \frac{n_g \sigma_{cx}(E)}{r^2 q} \int_a^b \frac{S(r'')}{\left| \frac{\partial \phi(r')}{\partial r'} \right|} \left[\frac{g(r', r'')}{1 - T_c^2 g_{cp}(r'')} \right] \Theta(r' - a) r''^2 dr'' + \frac{r''^2}{r^2} T_c \left[\frac{g(a, r'')}{1 - T_c^2 g_{cp}(r'')} \right] \left\{ 1 - \exp[n_g \sigma_{cx}(E)(r - a)] \right\} \frac{S(r'')}{q \left| \frac{\partial \phi(r'')}{\partial r''} \right|} \quad (65)$$

where r' in the integral is determined by Eq. (56) and r'' in the last term is determined by Eq. (62).

Similar to neutrals generated by class I ions, the inward traveling fast neutrals from class II ions cross the origin and become outward traveling fast neutrals. We also pick up a contribution from charge exchange of outward traveling ions with background gas. Starting with Eq. (55) for class I ions and making the replacements above to convert it to the corresponding equation for class II ions, we get

$$\delta \Gamma_{n2}^+(r, E) = \frac{r''^2}{r^2} T_c S(r'') dr'' \left[\frac{g(a, r'')}{1 - T_c^2 g_{cp}(r'')} \right] \left\{ 1 - \exp[-n_g \sigma_{cx}(E)(a + r)] \right\}. \quad (66)$$

We convert this to $f_{n2}^+(r, E)$ using Eqs. (61)- (63);

$$f_{n2}^+(r, E) = \frac{r''^2}{r^2} T_c \left[\frac{g(a, r'')}{1 - T_c^2 g_{cp}(r'')} \right] \left\{ 1 - \exp[n_g \sigma_{cx}(E)(r + a)] \right\} \frac{S(r'')}{q \left| \frac{\partial \phi(r'')}{\partial r''} \right|}. \quad (67)$$

We have to add the contribution from Eq. (59) for fast neutrals born in the intergrid region:

$$f_{n2}^+(r, E) = T_c \frac{n_g \sigma_{cx}(E)}{r^2 q} \int_a^b \frac{S(r'')}{\left| \frac{\partial \phi(r')}{\partial r'} \right|} \left[\frac{g(r', r'')}{1 - T_c^2 g_{cp}(r'')} \right] \Theta(r' - a) r''^2 dr'' + \frac{r''^2}{r^2} T_c \left[\frac{g(a, r'')}{1 - T_c^2 g_{cp}(r'')} \right] \left\{ 1 - \exp[n_g \sigma_{cx}(E)(r + a)] \right\} \frac{S(r'')}{q \left| \frac{\partial \phi(r'')}{\partial r''} \right|}. \quad (68)$$

As before, r' in the integral is determined by Eq. (56) and r'' in the last term is determined by Eq. (62).

Next we consider the outgoing neutrals in the intergrid region ($a < r < b$). The flux of fast neutrals just outside the cathode grid is

$$f_{n2}^+(a, E) = T_c^2 \frac{n_g \sigma_{cx}(E)}{a^2 q} \int_a^b \frac{S(r'')}{\left| \frac{\partial \phi(r')}{\partial r'} \right|} \left[\frac{g(r', r'')}{1 - T_c^2 g_{cp}(r'')} \right] \Theta(r' - a) r''^2 dr'' + \frac{r''^2}{a^2} T_c^2 \left[\frac{g(a, r'')}{1 - T_c^2 g_{cp}(r'')} \right] \left\{ 1 - \exp[2an_g \sigma_{cx}(E)] \right\} \frac{S(r'')}{q \left| \frac{\partial \phi(r'')}{\partial r''} \right|}. \quad (69)$$

The neutral flux coming through the cathode grid varies as r^{-2} due to spherical divergence;

$$f_{n2}^+(r, E) = \frac{a^2}{r^2} f_{n2}^+(a, E). \quad (70)$$

In addition to the flux of neutrals coming through the cathode grid, there will be a source due to charge exchange of outward traveling ions in the intergrid region. This source at radius r' produces a contribution to the flux at the radius r if $r' < r$. By the same arguments that lead to Eq. (58), the additional contribution to the outward traveling fast ions is

$$\delta f_{n2}^-(r, E) = \frac{n_g \sigma_{cx}(E)}{r^2 q} \int_a^r \frac{S(r'')}{\left| \frac{\partial \phi(r')}{\partial r'} \right|} \frac{g_{cp}(r'')}{g(r', r'') [1 - T_c^2 g_{cp}(r'')]} \Theta(r - r') r''^2 dr'', \quad (71)$$

so that the outward traveling fast neutral distribution in the intergrid region is

$$f_{n2}^+(r, E) = T_c^2 \frac{n_g \sigma_{cx}(E)}{r^2 q} \int_a^b \frac{S(r'')}{\left| \frac{\partial \phi(r')}{\partial r'} \right|} \left[\frac{1}{1 - T_c^2 g_{cp}(r'')} \right] \left[g(r', r'') \Theta(r' - a) + \frac{g_{cp}(r'')}{g(r', r'')} \Theta(r - r') \right] r''^2 dr'' + \frac{r''^2}{r^2} T_c^2 \left[\frac{g(a, r'')}{1 - T_c^2 g_{cp}(r'')} \right] \left\{ 1 - \exp[2an_g \sigma_{cx}(E)] \right\} \frac{S(r'')}{q \left| \frac{\partial \phi(r'')}{\partial r''} \right|}. \quad (72)$$

The total fast neutral energy distribution is simply the sum over the class I and class II contributions at each energy, and in each region,

$$f_n^\pm(r, E) = f_{n1}^\pm(r, E) + f_{n2}^\pm(r, E). \quad (73)$$

Finally we come to the region outside the anode, where there are no additional sources of fast neutrals. The flux drops by $1/r^2$ due to the spherical divergence;

$$f_n^+(r, E) = \frac{b^2}{r^2} T_a f_n^+(b, E) \quad (74)$$

$$f_n^+(r, E) = 0$$

where $f_n^+(b, E)$ is evaluated just inside the anode.

D. Cathode current

A difficulty with our model so far is that experiments do not normally provide a direct measurement of the ion flux, Γ_0 , crossing the anode and entering the intergrid region to use as the input to our analysis. However, the current to the cathode is normally measured experimentally. Consequently, we use the cathode current to determine Γ_0 . Within the context of our model, there are several contributions to the cathode current. The first is from class I ions crossing the anode, heading inward, and being intercepted by the cathode grid. The second is from class II ions born in the intergrid and cathode regions and intercepted by the cathode grid. These ions intercept the grid at finite energy and induce secondary electron emission; this also contributes to the measured cathode current. We allow for an energy- and species-dependent secondary electron emission coefficient, $\gamma_i(E)$. Cold ions produced in the cathode region ($r < a$), are contained by the electrostatic potential. Both the cold ions and the converging fast ions produce a positive potential relative to the cathode grid that can trap electrons. If the cold ions reach the cathode grid before being neutralized by the electrons trapped in the cathode region, they are neutralized at the grid surface and contribute to the cathode current. However, if they are neutralized by the trapped electrons, then they do not contribute to the cathode current. The trapped electron physics is beyond the scope of this paper, so we consider both extremes to “bracket” the results. Thermionic emission may also affect the measured cathode current; this depends on the cathode material and its operating temperature, and is outside the realm of this analysis.

The contribution from class I ions being intercepted by the cathode grid is

$$I_{c1} = 4\pi q(1 - T_c)\Gamma_0 b^2 \left[f(a) + T_c \frac{f^2(0)}{f(a)} \right] [1 + \gamma(qV_0)], \quad (75)$$

where $-V_0$ is the potential on the cathode. The first term in the square bracket in Eq. (75) is the contribution from ions hitting the outside of the cathode grid as they travel inward in radius, and the second term is the contribution from ions hitting the inside of the cathode grid as they travel outward in radius. The factor T_c appears to the first power inside the square brackets since the outward traveling ions have traversed the cathode grid once to get to the cathode region.

The second part of the cathode current is that due to ions being created in the region between the cathode and the anode (class II ions). This contribution is

$$I_{c2} = 4\pi q(1 - T_c) \int_a^b \frac{S(r')}{1 - T_c^2 g_{cp}(r')} \left[g(a, r') + T_c \frac{g_{cp}(r')}{g(a, r')} \right] [1 + \gamma(r')] r'^2 dr'. \quad (76)$$

The terms in the square bracket represent the inward and outward traveling ions, respectively, hitting the cathode wires, just as for class I ions. The secondary electron emission coefficient is an implicit function of r' through its energy dependence using Eq. (9).

The final contribution to the cathode current is the effect of charge exchange and ionization at radii less than the cathode radius. These ions are created cold and trapped in the electrostatic well; they reach $r > a$ only through very slow energy diffusion, so they wander around and eventually are either collected by the cathode or neutralized by trapped electrons. Both class I and class II ions contribute to the source of these cold ions. The flux of class I ions inside the cathode is

$$n(r) = \frac{b^2}{r^2} \Gamma_0 T_c \left[f(r) + \frac{f^2(0)}{f(r)} \right], \quad (77)$$

where the survival function, f , inside the cathode is given by Eq. (32). Computing the rate of

cold ion production by charge exchange and ionization and integrating over the cathode region ($r < a$) gives the number of cold ions produced per unit time by class I ions within the cathode region;

$$I_{c3} = 4\pi q n_g \sigma_{tot} [E(a)] b^2 \Gamma_0 T_c \int_0^a \left[f(r) + \frac{f^2(0)}{f(r)} \right] dr. \quad (78)$$

Because of the constant energy and the exponential variation of $f(r)$ inside the cathode, the integral can be done analytically. The result is

$$I_{c3} = 4\pi q n_g \frac{\sigma_{tot}(E_{max})}{\sigma_{cx}(E_{max})} b^2 \Gamma_0 T_c f(a) \left\{ 1 - \exp[-2n_g \sigma_{cx}(E_{max}) a] \right\}, \quad (79)$$

where $E_{max} = E(a)$ using Eq. (2). We neglect secondary electron emission induced by cold ions created within the cathode region since these ions hit the cathode at very low energy.

The rate of cold ion production by charge exchange and ionization inside the cathode region by class II ions is

$$S_i(r) = \frac{n_g T_c}{r^2} \int_a^b \frac{\sigma_{tot}[E(r, r')] S(r')}{1 - T_c^2 g_{cp}(r')} \left[g(r, r') + \frac{g_{cp}(r')}{g(r, r')} \right] r'^2 dr'. \quad (80)$$

Integrating this over the volume of the cathode region gives

$$I_{c4} = 4\pi q n_g T_c \int_0^a \int_a^b \frac{\sigma_{tot}(E(r, r')) S(r')}{1 - T_c^2 g_{cp}(r')} \left[g(r, r') + \frac{g_{cp}(r')}{g(r, r')} \right] r'^2 dr' dr. \quad (81)$$

Inside the cathode the energy is constant at $E(a, r')$, and the attenuation function $g(r, r')$ is given by Eq. (33). Consequently, we can reverse the order of the two integrations in Eq. (81) and do the r -integration analytically. The result is

$$I_{c4} = 4\pi q T_c \int_a^b r'^2 \frac{\sigma_{tot}[E(a, r')] S(r') g(a, r')}{\sigma_{cx}[E(a, r')] 1 - T_c^2 g_{cp}(r')} \left\{ 1 - \exp[-2n_g \sigma_{cx}[E(a, r')] a] \right\} dr'. \quad (82)$$

The total electron current to the cathode is then

$$I_c = I_{c1} + I_{c2} + I_{c3} + I_{c4}. \quad (83)$$

if the cold ions created in the cathode region are included in the cathode current. However, if the trapped electrons neutralize these ions before they reach the cathode grid, then the cathode current is simply

$$I_c = I_{c1} + I_{c2}. \quad (84)$$

E. Fusion Reaction Rate

The fusion reaction rate, which is a point of possible connection to experimental results, can be calculated using the energy spectrum given above. We consider two contributions to the fusion rate, (1) fast ions colliding with the background gas, and (2) fast neutral atoms colliding with the background gas. We neglect fusion due to ion-ion collisions since the plasma is weakly ionized. We also do not consider fusion due to fast ions or neutral atoms colliding with gas embedded in the grids or vacuum chamber wall, since this topic is outside the scope of this paper.

The fusion rate per unit volume due to fast ions colliding with the background gas can be determined from

$$S_{fi}(r) = n_g \int \sigma_f(E) \{f^+(r, E) + f^-(r, E)\} dE. \quad (85)$$

where $\sigma_f(E)$ is the relevant fusion cross section; the ion energy spectra, f^+ and f^- are given in Eqs. (28) and (29) for the intergrid region, and in Eqs. (30) and (31) for the cathode region. The fusion rate per unit volume due to fast neutral atoms colliding with the background gas can be determined from

$$S_{fn}(r) = n_g \int \sigma_f(E) \{f_n^+(r, E) + f_n^-(r, E)\} dE \quad (86)$$

where the relevant fast neutral atom energy spectra are given in Eq. (73), which uses results from the following equations: Eqs. (40) and (58) for inward traveling neutrals in the intergrid region, Eqs. (55) and (72) for outward traveling neutrals in the intergrid region, Eqs. (47) and (65) for inward traveling neutrals in the cathode region, Eqs. (51) and (68) for outward traveling neutrals in the intergrid region, and Eq. (74) for fast neutrals in the source region.

III. RESULTS

The formalism and analysis presented in Sec. II have been implemented in a computer code. As an example, we consider a ^3He plasma in a Wisconsin IEC device; the machine normally operates with a deuterium plasma, but has also utilized D- ^3He plasmas,²¹ and has been used for ^3He - ^3He studies.^{12,13} The vacuum vessel of the UW-IEC experiment consists of a large aluminum chamber 91 cm in diameter and 66 cm high; the base pressure is in the range 1×10^{-6} to 5×10^{-6} Torr, with the operating pressure normally between 1 and 4 mTorr. Different size cathode and anode grids have been studied; typical voltages on the cathode grid are between -30 kV and -185 kV, with the anode grid grounded.

As an example calculation to illustrate the predictions from this analysis, we consider a 20 cm diameter cathode and 40 cm diameter anode, cathode potential of 200 kV, cathode current of 60 mA, and operating helium pressure of 2 mTorr; cold ions produced in the cathode region are assumed to reach the cathode grid, and are therefore counted in the cathode current. For this case the attenuation function, $f(r)$, for class I ions and the complete pass probability, $g_{cp}(r)$, for class II ions is shown in Fig. 2. The cold ion source rate produced by class I ions, $A(r)$, and the

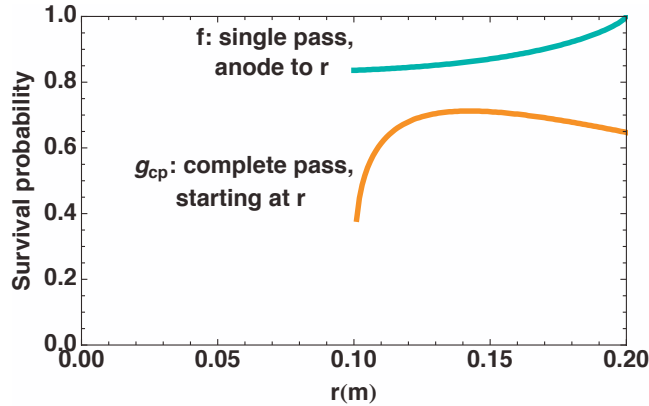


Figure 2. The attenuation function, $f(r)$, for class I ions and the complete pass probability, $g_{cp}(r)$, for class II ions for a case with $a=0.1$ m, $b=0.2$ m, $V_0=200$ kV, $I_c=60$ mA, $P=2$ mTorr.

solution to the Volterra integral equation, $S(r)$, are shown in Fig. 3; the peaking at the anode radius (20 cm) is due to the low energy of the ions at the anode and the resulting high charge exchange rate. The rise of $A(r)$ towards the cathode is due to the convergence of the ion motion in spherical geometry; the rise of $S(r)$ towards the center is partly due to the converging ion motion and to the accumulation of class II ions. Figure 4 shows the resulting ion and neutral atom energy spectra at the cathode. The ions have a broad energy spectrum due to charge

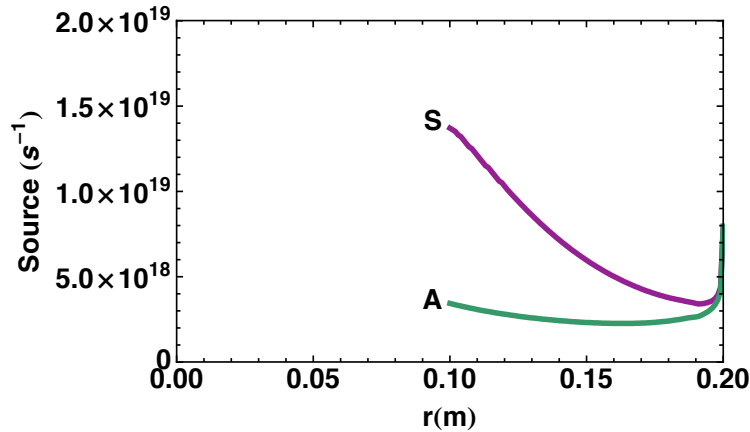


Figure 3. The cold ion source, $A(r)$, produced by class I ions, and the solution, $S(r)$, to the Volterra integral equation for a case with $a=0.1$ m, $b=0.2$ m, $V_0=200$ kV, $I_c=60$ mA, $P=2$ mTorr.

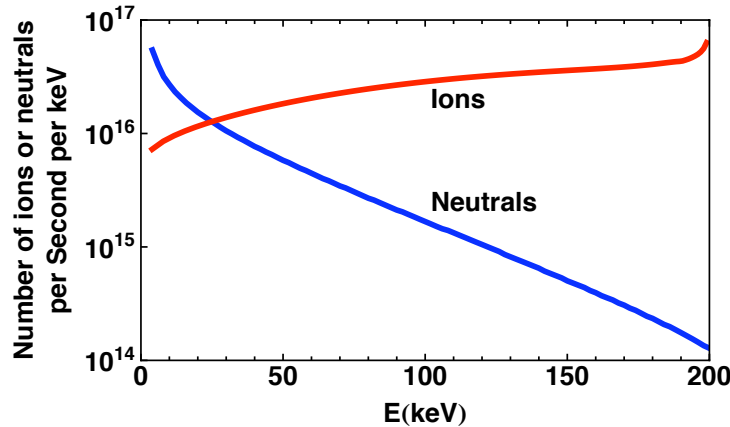


Figure 4. Ion and neutral atom energy spectra at the cathode radius for a case with $a=0.1$ m, $b=0.2$ m, $V_0=200$ kV, $I_c=60$ mA, $P=2$ mTorr.

exchange producing stationary ions that get accelerated by the electric field; not shown in Fig. 4 is the delta function spectrum at 200 kV of class I ions as they reach the cathode. The neutral atoms have an energy spectrum that peaks at low energy; this is due to the energy dependence of the charge exchange cross section. Figure 5 shows the ${}^3\text{He}-{}^3\text{He}$ fusion rate as a function of the

operating pressure; the increase with pressure is due to the increased target atom density and the rollover at higher pressure is due to softening of the ion and neutral energy spectra with increased operating pressure. Figure 6 shows the effect of increasing cathode voltage on the ${}^3\text{He}$ - ${}^3\text{He}$ fusion rate; not surprisingly, the fusion rate increases rapidly with increasing voltage. Figure 7 shows the effect of decreasing the anode radius while holding the cathode radius constant. Surprisingly, decreasing the anode radius greatly increases the fusion rate; the decreased separation increases the electric field, allowing the ions to reach higher energy before undergoing charge exchange with the background gas. This hardens both the ion and fast neutral atom energy spectra.

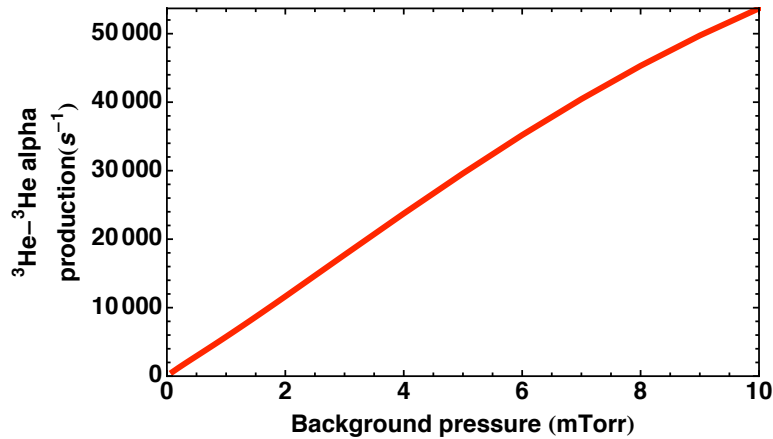


Figure 5. The ${}^3\text{He}$ - ${}^3\text{He}$ fusion rate as a function of the operating pressure for a case with $a=0.1$ m, $b=0.2$ m, $V_0=200$ kV, $I_c=60$ mA.

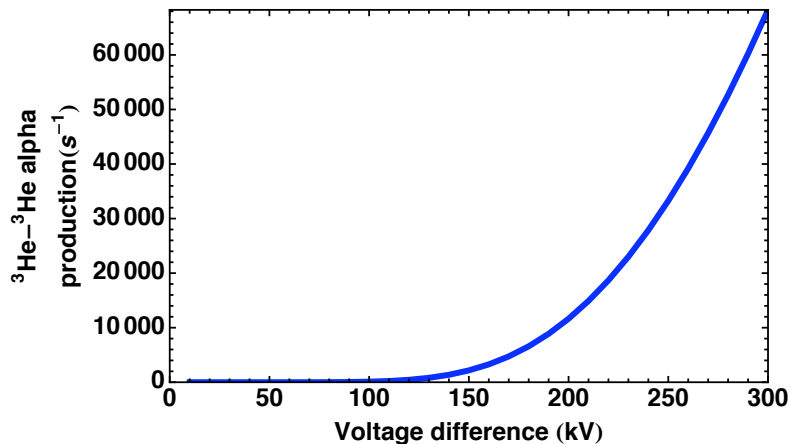


Figure 6. The effect of varying cathode voltage on the ${}^3\text{He}$ - ${}^3\text{He}$ fusion rate for a case with $a=0.1$ m, $b=0.2$ m, $I_c=60$ mA, $P=2$ mTorr.

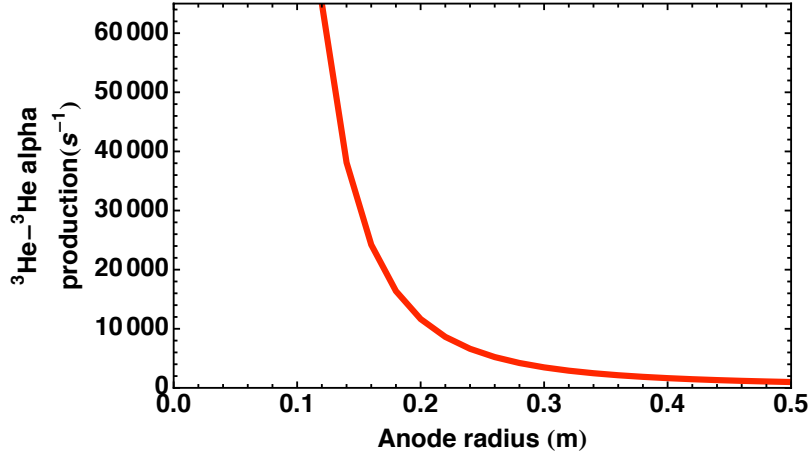


Figure 7. The effect on the ${}^3\text{He}-{}^3\text{He}$ fusion rate of varying the anode radius, while holding the cathode radius constant for a case with $a=0.1$ m, $V_0=200$ kV, $I_c=60$ mA, $P=2$ mTorr.

Unfortunately, experimental IEC data is only available for plasmas that involve molecular ions, so we cannot compare our analysis in this paper with actual data. Comparison between experiments and theory is deferred to the companion paper,¹⁴ which extends this analysis to multi-species plasmas involving D^+ , D_2^+ , and D_3^+ ions in a background D_2 gas.

IV. SUMMARY AND CONCLUSIONS

We have developed a formalism for analyzing the effect of ion-neutral gas interactions on the flow of ions between nearly transparent electrodes in spherical geometry; in this paper the formalism is restricted to neutral atoms and atomic ions, so that the important atomic effects are charge exchange and ion impact ionization. The formalism is applied to spherical, gridded, inertial-electrostatic confinement (IEC) devices. The formalism yields detailed predictions about the energy spectra of the ions and fast neutral atoms, and the resulting fusion rate for ${}^3\text{He}$ ions in a background ${}^3\text{He}$ gas. The results are illustrated with an example calculation for the Wisconsin IEC device operating on ${}^3\text{He}$. The analysis is useful for optimizing the performance of such devices, although experimental confirmation of the results is not yet available. In a companion paper, this formalism is extended to the more physically relevant case of molecular ions, such as deuterium ions in a deuterium gas, and compares the predictions with experimental results for the Wisconsin IEC device operating on deuterium.

ACKNOWLEDGMENTS

We gratefully acknowledge helpful discussions with the Wisconsin inertial-electrostatic confinement fusion experimental group. This research is supported by the U.S. Department of Energy Grant No. De-FG02-04ER54745.

REFERENCES

- ¹ C.D. Child, Phys. Rev. **32**, 492 (1911).
- ² I. Langmuir, Phys. Rev. **2**, 450 (1913).
- ³ I. Langmuir and K.B. Blodgett, Phys. Rev. **24**, 49 (1924).
- ⁴ D. Bohm, "Minimum Ionic Kinetic Energy for a Stable Sheath," Chapter 3 in A. Guthrie and R.K. Wakerling, eds., *Characteristics of Electrical Discharges in Magnetic Fields* (McGraw-Hill, New York, 1949).
- ⁵ S.A. Self, Phys. Fluids **6**, 1762 (1963).
- ⁶ G.A. Emmert, R.M. Wieland, A.T. Mense, and J.N. Davidson, Phys. Fluids **23**, 803 (1980).
- ⁷ J.T. Scheuer and G.A. Emmert, Phys. Fluids **31**, 1748 (1988).
- ⁸ R.C. Bissel, P.C. Johnson, and P.C. Stangeby, Phys. Fluids B **1**, 1133 (1989).
- ⁹ K.-U. Riemann, J. Physics D: Appl. Phys. **24**, 493 (1991).
- ¹⁰ L. Oksuz and N. Hershkowitz, Phys. Rev. Lett. **89**, 145001 (2002).
- ¹¹ K.-U. Riemann, Phys. Plasmas **4**, 4158 (1997).
- ¹² G.R. Piefer, J.F. Santarius, R.P. Ashley, and G.L. Kulcinski, Fusion Sci. Technol. **47**, 1255 (2005).
- ¹³ G.R. Piefer, Ph.D. Thesis, University of Wisconsin-Madison (2006).
- ¹⁴ G.A. Emmert and J.F. Santarius, "Atomic and Molecular Effects on Spherically Convergent Ion Flow II: Multiple Molecular Species" submitted to Phys. Plasmas.
- ¹⁵ W.C. Elmore, J.L. Tuck, and K.M. Watson, Phys. Fluids **2**, 239 (1959).
- ¹⁶ P.T. Farnsworth, "Electric Discharge Device for Producing Interactions between Nuclei," US Patent #3,258,402 (1966).
- ¹⁷ R. Hirsch, J. Appl. Phys. **38**, 4522 (1967).
- ¹⁸ G.H. Miley, Y. Gu, J.M. DeMora, R.A. Stubbers, T.A. Hochberg, J.H. Nadler, and R.A. Anderl, IEEE Trans. Plasma Sci. **25**, 733 (1997).
- ¹⁹ T.A. Thorson, R.D. Durst, R.J. Fonck, and L.P. Wainwright, Phys. Plasmas **4**, 4 (1997).
- ²⁰ T.A. Thorson, R.D. Durst, R.J. Fonck, and A.C. Sontag, Nuclear Fusion **38**, 495 (1998).
- ²¹ R.P. Ashley, G.L. Kulcinski, J.F. Santarius, S.K. Murali, and G. Piefer, Proc. 18th IEEE/NPSS Symposium on Fusion Engineering, 1999 (IEEE, Piscataway, New Jersey, 1999), p. 35.
- ²² J.H. Nadler, G.H. Miley, H. Momota, Y. Shaban, Y. Nam, and M. Coventry, Fusion Technol. Part 2, **39**, 492 (2001).
- ²³ K. Yoshikawa, K. Masuda, T. Takamatsu, E. Hotta, K. Yamauchi, S. Shiroya, T. Misawa, Y. Takahashi, M. Ohnishi, and H. Osawa, Fusion Sci. Technol. **52**, 1092 (2007).

- ²⁴ J.F. Santarius, G.L. Kulcinski, R.P. Ashley, D.R. Boris, B.B. Cipiti,, S. Krupakar Murali, G.R. Piefer, R.F. Radel, T.E. Radel, and A.L. Wehmeyer, *Fusion Sci. Technol.* **47**, 1238 (2005).
- ²⁵ A.L. Wehmeyer, R.F. Radel, and G.L. Kulcinski, *Fusion Sci. Technol.* **47**, 1260 (2005).
- ²⁶ G. L. Kulcinski, J. F Santarius, G. A. Emmert, et al., *Fusion Sci. Technol.* **56**, 493 (2009).
- ²⁷ R.A. Nebel, S. Stange, J. Park, J.M. Taccetti, S.K. Murali, and C.E. Garcia, *Phys. Plasmas* **12**, 012701 (2005).
- ²⁸ R.M. Meyer, Z.M. Smith, M.A. Prelas, and S.K. Loyalka, *Phys. Plasmas* **15**, 022105 (2008).
- ²⁹ R.F. Radel, G.L. Kulcinski, R.P. Ashley, J.F. Santarius, G.R. Piefer, D.R. Boris, R. Giar, B. Egle, C. Seyfert, S.J. Zenobia, and E. Alderson, *Fusion Sci. Technol.* **52**, 1087 (2007).
- ³⁰ G.L. Kulcinski, J.W. Weidner, B.B. Cipiti, R.P. Ashley, J.F. Santarius, S.K. Murali, G.R. Piefer, and R.F. Radel, *Fusion Sci. Technol.* **44**, 559 (2003).
- ³¹ G.L. Kulcinski and J.F. Santarius, *J. Fusion Energy* **17**, 17 (1998).
- ³² William H. Press, Brian R. Flannery, Saul A. Teukolsky, and William T. Vettering, in *Numerical Recipes in Fortran: The Art of Scientific Computing* (Cambridge Univ. Press, New York, NY, 1992), p. 786.